Triphenylphosphine-substituted Triruthenaborane Clusters: a Route to $[Ru_3(CO)_{9-x}(PPh_3)_xBH_5]$ (x = 1–3) *via* Systematic Cluster Degradation. Molecular Structures of $[Ru_3H(CO)_8(PPh_3)(B_2H_5)]$ and $[Ru_3(CO)_6(PPh_3)_3BH_5]\cdot CH_2Cl_2$†

Catherine E. Housecroft,*[a] Dorn M. Matthews,[a] Andrew J. Edwards[b] and Arnold L. Rheingold*[b]

[a] *University Chemical Laboratory, Lensfield Road, Cambridge CB2 1EW, UK*
[b] *Department of Chemistry, University of Delaware, Newark, DE 19716, USA*

Photolysis of a mixture of $[Ru_3H(CO)_9(B_2H_5)]$ and PPh_3 gives $[Ru_3H(CO)_8(PPh_3)(B_2H_5)]$ in good yield. Its molecular structure has been determined and the results confirm that it is a *nido* cluster related to pentaborane(9). Photolysis of $[Ru_3H(CO)_9(B_2H_5)]$ with an excess of PPh_3 and time > 4 h yields mono-, bis-and tris-(triphenylphosphine)-substituted $[Ru_3(CO)_9(BH_5)]$ *via* borane abstraction. The molecular structure of $[Ru_3(CO)_6(PPh_3)_3BH_5]\cdot CH_2Cl_2$ has been determined, confirming the presence of a tetrahedral Ru_3B core. In solution, the isomer preferences for members of the series $[Ru_3(CO)_{9-x}(PPh_3)_xBH_5]$ (x = 1–3) have been studied and it is observed that the distribution of *endo*-hydrogen atoms in $[Ru_3(CO)_{9-x}(PPh_3)_xBH_5]$ (x = 0–3) depends on x.

As part of a wider set of studies involving ruthenium–boron clusters we have reported results concerning two new compounds with cluster cores of composition Ru_3B[1] and Ru_3B_2.[2,3] The structure of $[Ru_3(CO)_9BH_5]$ **1** was proposed[1] from spectroscopic data and by analogy with the ferraborane $[Fe_3(CO)_9BH_5]$ which has been crystallographically characterised.[4] Initially, the structure of $[Ru_3H(CO)_9(B_2H_5)]$ **2** was also proposed[2] on the grounds of spectroscopic data. Owing to the difficulties we experienced in growing X-ray-quality crystals of either of **1** or **2**, we decided to prepare phosphine-substituted derivatives of them in the hope that they would crystallise more readily than the parent clusters. The reaction of **2** with PPh_3 under photolytic conditions did lead successfully to $[Ru_3H(CO)_8(PPh_3)(B_2H_5)]$ **3**, and we have reported the structure of this compound in a preliminary communication.[3] Phosphine-substituted derivatives of $[Ru_3(CO)_9BH_5]$ proved to be difficult targets to access under photolytic conditions because cluster expansion[5] competes significantly with substitution under these experimental conditions. We now report in full the synthesis and structural characterisation of $[Ru_3H(CO)_8(PPh_3)(B_2H_5)]$.[2] We also illustrate how the degradation of this cluster by treatment with an excess of PPh_3 provides a convenient route to a series of phosphine-substituted clusters of general formula $[Ru_3(CO)_{9-x}(PPh_3)_xBH_5]$ (x = 1–3) allowing more detailed studies of this cluster family to be carried out.

Experimental

General.—Fourier-transform NMR spectra were recorded on a Bruker WM 250 or AM 400 spectrometer: ^1H shifts are reported with respect to δ 0 for $SiMe_4$, ^{11}B with respect to δ 0 for $F_3B\cdot OEt_2$ and ^{31}P with respect to H_3PO_4. All downfield chemical shifts are positive. Infrared spectra were recorded on a Perkin Elmer FT 1710 spectrophotometer, FAB (fast atom bombardment) mass spectra in a 3-nitrobenzyl alcohol matrix.

† *Supplementary data available:* see Instructions for Authors, *J. Chem. Soc., Dalton Trans.*, 1993, Issue 1, pp. xxiii–xxviii.

All reactions were carried out under argon by using standard Schlenk techniques. Solvents were dried over suitable reagents and freshly distilled under N_2 before use. Separations were carried out by thin-layer plate chromatography with Kieselgel 60-PF-254 (Merck). The compound $[Ru_3H(CO)_9(B_2H_5)]$ was prepared as previously reported;[6] PPh_3 was used as received (Aldrich). Photolysis experiments used a mercury high-pressure lamp. Infrared spectral characteristics of the new compounds are collected in Table 1 and NMR spectroscopic data are given in Tables 2 and 3.

Preparations.—$[Ru_3H(CO)_8(PPh_3)(B_2H_5)]$ **3**. *Method* 1. Triphenylphosphine (13 mg, 0.05 mmol) dissolved in tetrahydrofuran (thf) (2.5 cm^3) was added to $[Ru_3H(CO)_9(B_2H_5)]$ **2** (29 mg, 0.05 mmol) in thf (1.0 cm^3). The resulting solution was photolysed for 2 h during which time it changed from yellow to orange. Separation of the products was achieved by TLC; eluting with hexane gave first a yellow fraction (unreacted **2**, ≈60% yield), secondly a yellow fraction, $[Ru_3H(CO)_8(PPh_3)(B_2H_5)]$ **3** (≈30% yield), and an orange fraction which remained on the baseline. This was further eluted with CH_2Cl_2–hexane (1:1) and two fractions were collected but in trace amounts only. They were identified from their spectral characteristics as $[Ru_4H_4(CO)_{10}(PPh_3)_2]$[7] and $[Ru_3H(CO)_7(PPh_3)_2(B_2H_5)]$ **4**. FAB mass spectra: **3**, P^+ at m/z 817 with eight CO losses (calc. for $^{12}C_{26}{}^1H_{21}{}^{11}B_2{}^{16}O_8{}^{31}P^{101}Ru_3$: m/z 817); **4**, P^+ at m/z 1052 with seven CO losses (calc. for $^{12}C_{43}{}^1H_{36}{}^{11}B_2{}^{16}O_7{}^{31}P_2{}^{101}Ru_3$: m/z 1051).

Method 2. Triphenylphosphine (26 mg, 0.10 mmol) dissolved in CH_2Cl_2 (2.5 cm^3) was added to $[Ru_3H(CO)_9(B_2H_5)]$ **2** (58 mg, 0.10 mmol) in CH_2Cl_2 (2.5 cm^3). The resulting solution was stirred at room temperature for 3.5 d during which it changed from yellow to orange. Separation by TLC and eluting with hexane yielded, first unreacted **2** (≈50%), then yellow $[Ru_3H(CO)_8(PPh_3)(B_2H_5)]$ **3** (≈20%), and finally yellow $[Ru_4H_4(CO)_{11}(PPh_3)]$[7] (≈20%). A narrow orange band remained on the baseline and this was not separated further.

$[Ru_3(CO)_{9-x}(PPh_3)_xBH_5]$ (x = 1–3). Triphenylphosphine (73 mg, 0.28 mmol) dissolved in thf (2.5 cm^3) was added to

$[Ru_3H(CO)_9(B_2H_5)]$ **2** (41 mg, 0.07 mmol) previously dissolved in thf (1.0 cm^3). The resulting solution was photolysed for 16 h, changing from yellow to orange. Products were separated by TLC; eluting with hexane gave four yellow fractions and a significant orange baseline residue: first unreacted compound **2** in trace amounts only, secondly $[Ru_3(CO)_8(PPh_3)BH_5]$ **5** (≈5%), thirdly a mixture of $[Ru_4H_4(CO)_{11}(PPh_3)]$[7] and $[Ru_4H(CO)_{11}(PPh_3)(BH_2)]$[8] (≈5%) and fourthly $[Ru_3H(CO)_8(PPh_3)(B_2H_5)]$ **3** (≈10%). After collection of these fractions, the eluting solvent was changed to CH_2Cl_2–hexane (1:2) and further separation yielded five further products, all yellow-orange: in order of elution, $[Ru_3(CO)_7(PPh_3)_2BH_5]$ **6** (≈5%), $[Ru_4H_4(CO)_{10}(PPh_3)_2]$[7] (≈15%), $[Ru_4H(CO)_{10}(PPh_3)_2(BH_2)]$[8] (≈5%), $[Ru_3H(CO)_7(PPh_3)_2(B_2H_5)]$ **4** (≈15%) and $[Ru_3(CO)_6(PPh_3)_3BH_5]$ **7** (≈15%). Several other weak fractions having low retention values were not collected. FAB mass spectra: **5**, P^+ at *m/z* 805 with eight CO losses (calc. for $^{12}C_{26}{}^1H_{20}{}^{11}B^{16}O_8{}^{31}P^{101}Ru_3$: *m/z* 805); **6**, P^+ at *m/z* 1041 with seven CO losses (calc. for $^{12}C_{43}{}^1H_{35}{}^{11}B^{16}O_7{}^{31}P_2{}^{101}Ru_3$: *m/z* 1039); **7**, P^+ at *m/z* 1274 with seven CO losses (calc. for $^{12}C_{60}{}^1H_{50}{}^{11}B^{16}O_6{}^{31}P_3{}^{101}Ru_3$: *m/z* 1273).

Crystal Structure Determinations.—General. Crystallographic data for compounds **3** and **7** are collected in Table 4. Crystals were mounted on glass fibres with epoxy cement. Photographic characterisation and cell-reduction routines revealed no symmetry higher than triclinic in either case. Semiempirical corrections for absorption were applied using ψ-scan data. The structures were solved by direct methods which located the Ru atoms. All non-hydrogen atoms were refined with anisotropic thermal parameters, and hydrogen atoms were treated as idealised contributions with these exceptions: in **3** the borane hydrogen atoms were not located and were ignored, whilst in **7** the five hydrogen atoms associated with the central cluster were located and isotropically refined. In **7** the phenyl rings were constrained to rigid planar hexagons. All computations used the SHELXTL (4.2) library of programs.[9]

Additional material available from the Cambridge Crystallographic Data Centre comprises H-atom coordinates, thermal parameters and remaining bond lengths and angles.

Results and Discussion

The reactions of $[Ru_3H(CO)_9(B_2H_5)]$ **2** under varying conditions (see Experimental section) with PPh_3 lead to two series of phosphine-substituted clusters. Members of the first series are derived directly from **2** and are $[Ru_3H(CO)_8(PPh_3)(B_2H_5)]$ **3** and $[Ru_3H(CO)_7(PPh_3)_2(B_2H_5)]$ **4**. The compounds that comprise the second series are $[Ru_3(CO)_8(PPh_3)BH_5]$ **5**, $[Ru_3(CO)_7(PPh_3)_2BH_5]$ **6** and $[Ru_3(CO)_6(PPh_3)_3BH_5]$ **7**, and these are formed by selective degradation of members of the first series of clusters. The structural characterisations of compounds **3** and **7** reported below provide the first confirmation of clusters with Ru_3B_2 or Ru_3B cores.

Structural Confirmation of an Ru_3B_2 *Cluster.*—The triruthenaborane cluster **2** was first reported in 1977 but was not fully characterised.[10] More recently, we have prepared it and proposed that the compound is a structural analogue of B_5H_9 with three $\{Ru(CO)_3\}$ units replacing three $\{BH\}$ fragments,[2] being a member of the series of *nido* clusters $\{ML_n\}_x\{BH\}_{5-x}H_4$ (M = transition metal; ML_n = two-electron cluster fragment).[11–18] However, we have been unable to confirm the structure of **2** by single-crystal X-ray diffraction. The substitution of a carbonyl ligand by triphenylphosphine produced the derivative $[Ru_3H(CO)_8(PPh_3)(B_2H_5)]$ **3**, which readily crystallised. A crystal of **3** suitable for X-ray diffraction was grown from CH_2Cl_2 layered with hexane. The molecular structure is shown in Fig. 1, atomic coordinates are given in Table 5, and selected bond distances and angles in Table 6. The Ru_3B_2-cluster core of **3** is a distorted square pyramid; the three

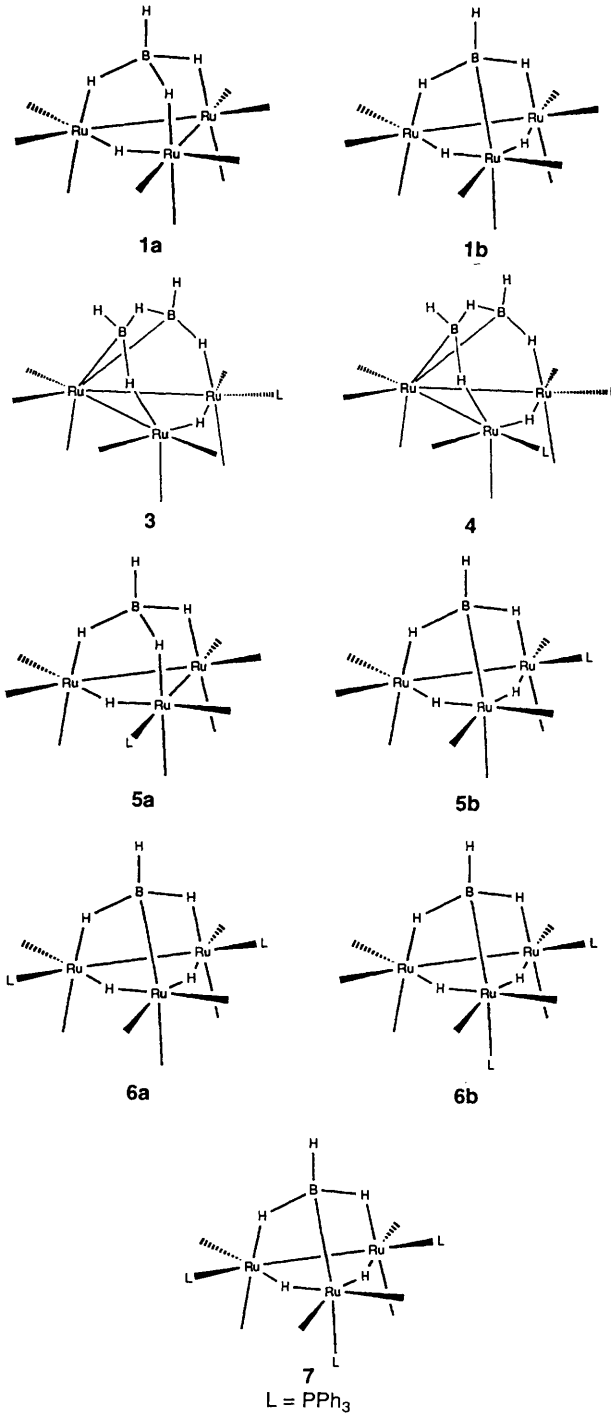

ruthenium atoms form one triangular face with one metal atom in the apical site of the square-pyramidal framework and two in adjacent basal sites. The PPh_3 substituent resides in an equatorial site on one of the basal ruthenium atoms. The carbonyl ligands are all terminal and are unexceptional. The Ru_3 frame is close to being an isosceles triangle with the edge Ru(1)–Ru(3) [3.009(1) Å] being significantly longer than Ru(1)–Ru(2) [2.758(1) Å] and Ru(2)–Ru(3) [2.767(1) Å]. These differences in distances and the observation that the carbonyl ligands on atoms Ru(1) and Ru(3) bend away from the Ru(1)–Ru(3) vector are consistent with the placement of a bridging hydrogen atom along Ru(1)–Ru(3).

None of the *endo*-hydrogen atoms was located directly in the structural analysis of compound **3**, but a consideration of the structural details in addition to NMR spectroscopic data allow

Table 1 Infrared spectroscopic data for compounds **1**–**7**; all samples as hexane solutions

Compound	ν_{CO}/cm^{-1}	Ref.[a]
1 $[Ru_3(CO)_9BH_5]$	2105w, 2075vs, 2051s, 2033s, 2020s	*b*
2 $[Ru_3H(CO)_9(B_2H_5)]$	2108w, 2082s, 2061(sh), 2055vs, 2042m, 2031m, 2012w, 1997w	2,6
3 $[Ru_3H(CO)_8(PPh_3)(B_2H_5)]$	2089m, 2053vs, 2044m, 2033s, 2021m, 1996m, 1991w	*c*
4 $[Ru_3H(CO)_7(PPh_3)_2(B_2H_5)]$	2074w, 2061vs, 2028s, 2020s, 1999m, 1979m	
5 $[Ru_3(CO)_8(PPh_3)BH_5]$	2086m, 2067s, 2050s, 2029vs, 2016vs, 1999m(sh), 1995m, 1980w(sh), 1975w	
6 $[Ru_3(CO)_7(PPh_3)_2BH_5]$	2075m, 2069m, 2039vs, 2022s, 2003vs, 1992m, 1985s, 1963m	
7 $[Ru_3(CO)_6(PPh_3)_3BH_5]$	2034s, 2015s, 1994w, 1975vs, 1955m	

[a] This work unless stated otherwise. [b] Ref. 1 gives spectral data for a solution in CH_2Cl_2. [c] Also ref. 3.

Table 2 128 MHz ^{11}B-$\{^1H\}$ and 162 MHz ^{31}P NMR spectroscopic data for compounds **1**–**7**; all samples as $CDCl_3$ solutions at 298 K except where stated

Compound	$\delta(^{11}B\text{-}\{^1H\})$	$\delta(^{31}P)$	Ref.[a]
1a[b]	+2.8	—	1
1b[b]	+21.0	—	1
2	+17.0	—	2, 6
3	+17.6, +14.8 (1:1)	+33.8	*c*
4	+15.3	+33.5	
5a (major isomer)	+6.0	+32.5	
5b (minor isomer)	+23.5	+35.1	
6a (major isomer)	+23.0	+32.6	
6b (minor isomer)	+23.0	+34.9, +26.6 (1:1)	
7	+23.3	+32.8, +26.3 (2:1)	

[a] This work except where indicated. [b] In CD_2Cl_2 at 298 K. [c] Also ref. 3.

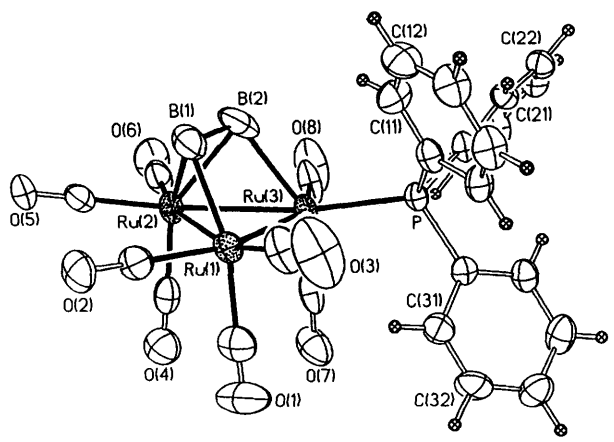

Fig. 1 Molecular structure of $[Ru_3H(CO)_8(PPh_3)(B_2H_5)]$ **3**. Hydrogen atoms were not located

the four *endo*-hydrogen atoms to be placed along the four edges of the square base of the pyramidal cluster core. In the high-field part of the ^1H NMR spectrum a doublet at δ −18.3 (J_{PH} = 14 Hz) is consistent with a *cis* relationship between the metal hydride and phosphorus atom[19] and therefore supports the conclusion drawn from the structural results, *i.e.* a bridging hydride ligand along edge Ru(1)–Ru(3). The B–B distance of 1.84(2) Å lies in the expected range for a boron–boron edge bridged by a hydrogen atom; its presence is supported by a resonance in the ^1H NMR spectrum at δ −1.2. The ^1H NMR shifts for the remaining two cluster-bound hydrogen atoms are indicative of Ru–H–B bridging character and the H atoms are placed along edges Ru(1)–B(1) and Ru(3)–B(2), thereby giving a structure for **3** which is analogous with that of B_5H_9.[20]

It is pertinent that the core of compound **3** (and similarly of **2** and **4**) can be considered in terms of a *nido* structure derived from an octahedron or can be regarded in terms of a B_2 unit interacting with an Ru_3-triangular framework. The latter suggests an analogue of a triruthenium-supported unsaturated hydrocarbon.[2] Both descriptions are useful when it comes to discussing the chemistry of the molecule.

Structural Confirmation of an Ru_3B *Cluster*.—The compound $[Ru_3(CO)_6(PPh_3)_3BH_5]$ **7** is the first crystallographically characterised cluster with an Ru_3B core; related iron and osmium compounds have been characterised.[4,21–23] The molecular structure of **7** is shown in Fig. 2; atomic coordinates are listed in Table 7, and selected distances and angles in Table 8. Cluster **7** possesses an approximate mirror plane passing through atoms Ru(2) and B(7) and the midpoint of Ru(1)–Ru(3). The boron atom caps the Ru_3 triangle being directly bonded to Ru(2) and indirectly *via* hydrogen-atom bridges to atoms Ru(1) and Ru(3). The disposition of ligands at each of the ruthenium centres is consistent with the presence of bridging hydrogen atoms along edges Ru(3)–B(7), Ru(1)–B(7), Ru(1)–Ru(2) and Ru(2)–Ru(3) and these have been located directly. One PPh_3 ligand is attached to each of atoms Ru(1) and Ru(3) and these two phosphine ligands are related by the approximate mirror plane; each PPh_3 ligand lies in an equatorial position. The unique phosphine ligand is axially co-ordinated to atom Ru(2). A single terminal hydrogen atom was found on the boron atom. The {BH} fragment is isolobal with an $\{Ru(CO)_3\}$ unit, and thus **7** is an analogue of $[Ru_4H_4(CO)_{12}]$.

Solution Spectroscopic Characterisation of Compounds **3** *and* **4**.—In solution the multinuclear NMR spectroscopic properties (Tables 2 and 3) of the monophosphine-substituted derivative, **3** are consistent with the presence of a single isomer with a structure equivalent to that observed in the solid state (Fig. 1). The phosphine ligand is in an equatorial site and is related to each of one Ru–H–B and one Ru–H–Ru bridging hydrogen atoms in a *cis* arrangement. The second phosphine ligand is introduced in a position that is symmetry related to the first to give compound **4**. There is no evidence for the presence of any other isomer for **4**.

Solution Spectroscopic Characterisation of Compounds **5**–**7**.—It is instructive to begin this discussion with comments concerning the isomerism observed for $[Ru_3(CO)_9BH_5]$.[1] In solution, $[Ru_3(CO)_9BH_5]$ exhibits two isomers, **1a** and **1b**, which are approximately equally populated; the isomerism arises from the relative positions of the bridging hydrogen atoms on the Ru_3B-cluster core. The two isomers are readily distinguished, not only by their characteristic ^1H NMR spectroscopic data (Table 3), but also by their ^{11}B NMR spectral shifts (Table 2). It has been noted that ^{11}B NMR shifts are sensitive to environment.[24] The ^{11}B NMR resonance for **1a**

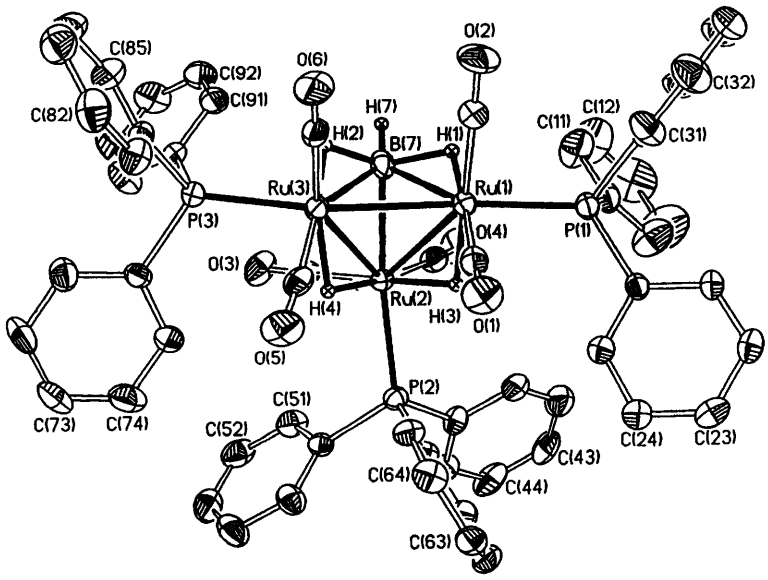

Fig. 2 Molecular structure of $[Ru_3(CO)_6(PPh_3)_3BH_5]$ **7**

Table 3 400 MHz ^1H NMR spectroscopic data for compounds **1**–**7**; all samples as $CDCl_3$ solutions at 298 K except where stated

Compound	δ(^1H)	Ref.[a]
1a[b]	+3.5 (br, 1 H, BH_{term}), −11.0 (br, 1 H, Ru–H–B), −12.2 (br, 2 H, Ru–H–B), −18.8 (s, 1 H, Ru–H–Ru)	1
1b[b]	+4.0 (br, 1 H, BH_{term}), −11.3 (br, 2 H, Ru–H–B), −18.4 (s, 2 H, Ru–H–Ru)	
2	+4.5 (br, 2 H, BH_{term}), −1.2 (br, 1 H, B–H–B), −12.3 (br, 2 H, Ru–H–B), −19.0 (s, 1 H, Ru–H–Ru)	2, 6
3	+7.55–7.20 (m, 15 H, Ph), +4.6 (br, 1 H, BH), +4.1 (br, 1 H, BH), −1.2 (br, 1 H, B–H–B), −11.2 (br, 1 H, Ru–H–B), −12.1 (br, 1 H, Ru–H–B), −18.3 (d, J_{PH} = 14 Hz, Ru–H–Ru)	*c*
4	+7.75–6.94 (m, 30 H, Ph), +4.6 (br, BH), −1.3 (br, 1 H, B–H–B), −11.2 (br, 2 H, Ru–H–B), −16.7 (unresolved m, 1 H, Ru–H–Ru)	
5a[d] (major isomer)	+7.55–7.26 (m, 15H, Ph), +4.3 (br, BH), −10.8 (br, 1 H, Ru–H–B), −11.6 (br, 1 H, Ru–H–B), −12.4 (br, 1 H, Ru–H–B), −18.21 (unresolved m, 1 H, Ru–H–Ru)	
5b[d] (minor isomer)	+7.55–7.26 (m, 15H, Ph), +4.3 (br, BH), −10.7 (br, 1 H, Ru–H–B), −11.1 (br, 1 H, Ru–H–B), −17.94 (unresolved m, 1 H, Ru–H–Ru), −18.18 (unresolved m, 1 H, Ru–H–Ru)	
6a (major isomer)	+7.72–7.05 (m, 30 H, Ph), +4.5 (vbr BH), −10.3 (br, 2 H, Ru–H–B), −17.69 (m, 2 H, Ru–H–Ru)	
6b (minor isomer)	+7.72–7.05 (m, 30 H, Ph), +4.5 (vbr BH), −10.3 (br, 1 H, Ru–H–B, see text), −11.0 (br, 1 H, Ru–H–B), −17.00 (m, 1 H, Ru–H–Ru), −17.13 (m, 1 H, Ru–H–Ru)	
7	+7.44–7.10 (m, 45 H, Ph), +4.4 (br, 1 H, BH), −10.4 (br, 2 H, Ru–H–B), −16.63 (m, 2 H, Ru–H–Ru)	

[a] This work except where indicated. [b] In CD_2Cl_2 at 233 K. [c] Also ref. 3. [d] In CD_2Cl_2 at 185 K (see text).

(δ +2.8) is diagnostic of the presence of one terminal B–H and three B–H–Ru interactions; for **1b**, the more downfield nature of the ^{11}B NMR signal at δ +21.0 is diagnostic of one terminal B–H, one direct B–Ru, and two B–H–Ru interactions.[1]

An inspection of the ^{11}B NMR spectroscopic data in Table 2 shows that for all members of the series $[Ru_3(CO)_{9-x}(PPh_3)_xBH_5]$ **5**–**7** the shift values fall into one of the two regions observed for **1a** and **1b** and, consistent with the ^1H NMR spectroscopic data (Table 3), suggest that the structures of the phosphine-substituted compounds are based on one or both of the isomeric Ru_3BH_5 skeletons observed for **1a** and **1b**. The structural characterisation of **7** confirms the arrangement of the cluster-bound hydrogen atoms previously proposed for **1b**.[1] In solution, **7** shows a preference for this one arrangement of bridging hydrogen atoms and the ^{11}B NMR spectra shift of δ +23.3 is close to that observed for **1b** (δ +21.0). The ^{31}P NMR spectrum exhibits two resonances, δ +32.8 (integral 2) and +26.3 (1). These signals correspond, respectively, to the equatorial phosphine ligands on atoms Ru(1) and Ru(3) and the unique axially substituted ligand on Ru(2) (Fig. 2) and, as will be seen below, the shifts are diagnostic of these particular environments. The unique phosphine ligand lies *cis* to two Ru–H–Ru bridging hydrogen atoms, whilst the two equatorially substituted ligands are *cis* to one Ru–H–Ru and *cis* to one Ru–H–B hydrogen atom.

Each of the disubstituted compound **6** and monosubstituted **5** exhibits two isomers in solution and the spectroscopic data described for **1** and **7** aid in the assignment of these isomers. The ^{31}P and ^1H NMR spectroscopic data (Tables 2 and 3) for **6** are consistent with the presence of two isomers in solution. However, the presence of a single ^{11}B NMR resonance (Table 2) implies that each possesses the same arrangement of cluster-bound hydrogen atoms. Thus, isomerism is a consequence of the positions of the phosphine ligands. For the major isomer, **6a**, ^1H and ^{31}P NMR spectral data indicate that a plane of symmetry is retained. It is a reasonable assumption that the two ligands are associated with different metal atoms. The ^{31}P NMR chemical shift value of δ +32.6 is, by comparison with the data for **7**, consistent with substitution at the sites shown in structure **6a**. The minor isomer, **6b**, has lost the plane of symmetry present in the unsubstituted parent compound **1b**. This feature along with the presence of two ^{31}P NMR spectral resonances (1 : 1), and by comparison with the structure of **7**, allow the structure drawn to be proposed for **6b**. Significantly, it is suggested that the preferred sites of phosphine substitution in both isomers of the disubstituted compound **6** mimic two of the sites confirmed crystallographically for the trisubstituted compound **7**.

The monophosphine-substituted derivative **5** exhibits two isomers in solution, but, unlike **6**, they are primarily a result of the arrangement of the cluster hydrogen atoms. For the major isomer, **5a**, the Ru–H–B region of the ^1H NMR spectrum shows three broad resonances integrating 1 : 1 : 1 and the shift of the ^{31}P resonance (δ +32.5) indicates equatorial substitution in a site that is *cis* to each of an Ru–H–B and Ru–H–Ru bridging

Table 4 Crystallographic data* for $[Ru_3H(CO)_8(PPh_3)(B_2H_5)]$ **3** and $[Ru_3(CO)_6(PPh_3)_3BH_5]$ **7**

	3	**7**
(*a*) Crystal parameters		
Formula	$C_{26}H_{21}B_2O_8PRu_3$	$C_{60}H_{50}BO_6P_3Ru_3{\cdot}CH_2Cl_2$
M	817.2	1358.9
Crystal dimensions/mm	0.22 × 0.22 × 0.28	0.42 × 0.23 × 0.14
a/Å	10.947(3)	10.882(2)
b/Å	12.596(5)	14.172(3)
c/Å	12.758(4)	20.401(4)
α/°	63.49(3)	78.18(1)
β/°	72.66(2)	89.54(2)
γ/°	86.46(3)	72.01(2)
U/Å^3	1497.4(6)	2924.2(12)
D_c/g cm^{-3}	1.813	1.543
μ(Mo-Kα)/cm^{-1}	15.91	9.88
F(000)	784	1364
(*b*) Data collection		
2θ scan range/°	4–55	4–48
Data collected (*h*,*k*,*l*)	−13 to 13, −16 to 14, −16 to 0	−12 to 12, −15 to 16, 0 to 23
	6955	
Reflections collected	6663	9483
Independent reflections	4406	9192
Independent observed reflections [$F_o > 4\sigma(F_o)$]	0.73, 0.61	6796
Maximum, minimum transmission		0.36, 0.32
(*c*) Refinement		
R	0.0695	0.0400
R'	0.0819	0.0471
Δ/σ_{max}	0.004	0.048
Δρ/e Å^{-3}	1.67	1.20
N_o/N_v	11.9	9.9
Goodness of fit	1.63	1.02
Weighting scheme, w^{-1}	$\sigma^2(F) + 0.0010\,F^2$	$\sigma^2(F) + 0.008\,F^2$

* Details in common: triclinic, space group $P\bar{1}$; $Z = 2$; crystal colour, yellow; Siemens P4 diffractometer; Mo-Kα radiation (λ = 0.710 73 Å); 278 K.

Table 5 Atomic coordinates (× 10^4) for $[Ru_3H(CO)_8(PPh_3)(B_2H_5)]$ **3**

Atom	*x*	*y*	*z*	Atom	*x*	*y*	*z*
Ru(1)	975(1)	6 894(1)	6 226(1)	C(7)	3 758(10)	8 684(13)	5 673(10)
Ru(2)	2 520(1)	5 736(1)	7 685(1)	C(8)	5 512(11)	7 121(13)	5 514(10)
Ru(3)	3 848(1)	7 390(1)	5 331(1)	C(11)	3 236(11)	6 790(10)	2 875(10)
P	4 425(2)	8 485(2)	3 172(2)	C(12)	2 467(12)	6 375(12)	2 428(12)
B(1)	1 735(15)	5 076(15)	6 632(14)	C(13)	1 896(11)	7 185(12)	1 589(11)
B(2)	3 493(19)	5 365(16)	6 093(14)	C(14)	2 070(10)	8 348(12)	1 231(10)
O(1)	604(10)	9 093(10)	6 674(13)	C(15)	2 861(10)	8 791(10)	1 673(9)
O(2)	−1 423(7)	5 563(8)	8 328(8)	C(16)	3 416(8)	7 971(10)	2 520(8)
O(3)	−313(11)	7 787(14)	4 207(11)	C(21)	6 316(9)	8 202(8)	1 280(9)
O(4)	2 122(9)	7 615(9)	8 640(9)	C(22)	7 581(10)	8 245(9)	578(10)
O(5)	594(8)	3 821(8)	9 883(7)	C(23)	8 578(10)	8 513(10)	865(10)
O(6)	4 808(9)	4 764(9)	8 633(9)	C(24)	8 338(9)	8 763(11)	1 840(10)
O(7)	3 690(9)	9 496(10)	5 906(9)	C(25)	7 086(9)	8 730(10)	2 559(9)
O(8)	6 488(8)	6 935(12)	5 634(9)	C(26)	6 065(8)	8 439(9)	2 268(8)
C(1)	772(10)	8 275(13)	6 535(13)	C(31)	3 112(10)	10 462(10)	3 160(10)
C(2)	−533(10)	6 059(10)	7 555(11)	C(32)	2 896(11)	11 602(11)	2 736(12)
C(3)	175(11)	7 458(14)	4 942(13)	C(33)	3 789(11)	12 483(11)	1 733(12)
C(4)	2 278(10)	6 945(11)	8 259(11)	C(34)	4 898(11)	12 119(11)	1 155(11)
C(5)	1 321(11)	4 537(11)	9 068(11)	C(35)	5 102(9)	10 927(10)	1 593(9)
C(6)	3 958(12)	5 136(11)	8 283(10)	C(36)	4 206(9)	10 072(8)	2 592(8)

hydrogen atom (see above). The ^{1}H NMR spectrum of the minor isomer, **5b**, illustrates that all four bridging hydrogen atoms are inequivalent. The ^{31}P NMR spectral shift (Table 2) implies that, as in **5a**, the PPh_3 ligand is related to each of an Ru–H–B and Ru–H–Ru bridging hydrogen atom in a *cis* fashion.

The structures proposed for compounds **5a**, **5b**, **6a** and **6b**, and confirmed for **7**, illustrate the following three points. First, as the value of *x* increases from 0 to 3 in the series $[Ru_3(CO)_{9-x}(PPh_3)_xBH_5]$ there is a tendency for the cluster-bound hydrogen atoms to migrate from the B–H–Ru to Ru–H–Ru bridging sites. However, we have not observed an isomer in which there are three Ru–H–Ru interactions. Secondly, two particular environments appear to be preferred for phosphine substitution: (*i*) mutually *trans* to a direct Ru–B interaction and *cis* to two Ru–H–Ru bridges, or (*ii*) *cis* to each of an Ru–H–B and Ru–H–Ru interaction. Note that case (*ii*) also holds for the sites of substitution in **3** and **4**. Thirdly, in the unsubstituted cluster **1a**, a fluxional process renders all three Ru–H–B hydrogen atoms equivalent at 298 K on the ^{1}H NMR spectroscopic time-scale;[1] in the related compound **5a** the system is static on the same time-scale although the ^{1}H NMR spectrum is better resolved at temperatures lower than 298 K (Table 3).

Mechanism of Cluster Substitution and Degradation.—The conversion of the Ru_3B_2- into Ru_3B-based clusters implies the removal of a monoborane unit and indeed during spectral monitoring of the reaction of **2** with PPh_3 the formation of the adduct $Ph_3P{\cdot}BH_3$ is observed [$\delta(^{11}B)$ − 35.8 (d), J_{PB} = 55 Hz]. The formal conversion of $[Ru_3H(CO)_9(B_2H_5)]$ into $[Ru_3(CO)_{9-x}(PPh_3)_xBH_5]$ (x = 1–3) and $Ph_3P{\cdot}BH_3$ clearly requires the addition of two hydrogen atoms, but it is expected that adventitious hydrogen atoms are available in the reaction system since there is evidence for cluster fragmentation and aggregation; both $[Ru_4H_4(CO)_{12-x}(PPh_3)_x]$ (x = 1 or 2) and $[Ru_4H(CO)_{12-x}(PPh_3)_x(BH_2)]$ (x = 1 or 2) are formed (see Experimental section).

In contrast to the prolonged photolysis of compound **2** with a four-fold excess of PPh_3, the stoichiometric reaction carried out over 2 h yields, essentially, only the monosubstituted compound **3** in addition to unreacted starting material. Degradation to members of the family $[Ru_3(CO)_{9-x}(PPh_3)_xBH_5]$ (x = 1–3) represents a very minor pathway. This implies that the removal of a BH_3 unit from **2** is not a facile process, and thus **2** is probably not the direct precursor to the $[Ru_3(CO)_{9-x}(PPh_3)_xBH_5]$ clusters. This suggests that phosphine substitution at **2** occurs *before* cluster degradation commences (Scheme 1). Consistent with this is the fact that no unsubstituted **1** was ever isolated as a product from the reactions studied.

In order to probe the mechanism of reaction further, the monosubstituted compound **3** was prepared and purified, and then used in a reaction (5 h photolysis in $[^2H_8]$thf) with an excess of PPh_3. The reaction was continually monitored by ^{11}B and ^1H NMR spectroscopy. A disadvantage of monitoring by ^{11}B NMR spectroscopy is the coincidence of resonances for **5b**, **6** and **7**, and the near coincidence (in $[^2H_8]$thf) of the signal for **4** with those of **5b**, **6** and **7**. (The ^{11}B NMR shifts are quite sensitive to solvent [25]). However, as the Ru_3B_2 core of **3** and/or **4** is degraded to clusters containing the Ru_3B core, the formation of the latter should approximately mimic the growth of the adduct $Ph_3P{\cdot}BH_3$ and use can be made of this partially to partition the integral of the signal for compounds **4**–**7**. Fig. 3 shows the decay of **3**, the growth of Ru_3B-based products, and the growth and subsequent decay of **4** as recorded from ^{11}B NMR spectroscopic data over the 5 h reaction period. The

Table 6 Selected bond distances (Å) and angles (°) for $[Ru_3H(CO)_8(PPh_3)(B_2H_5)]$ **3**

Ru(1)–Ru(2)	2.758(1)	Ru(1)–Ru(3)	3.009(1)
Ru(2)–Ru(3)	2.767(1)	Ru(1)–B(1)	2.27(2)
Ru(2)–B(1)	2.24(2)	Ru(3)–B(2)	2.30(2)
Ru(2)–B(2)	2.23(2)	B(1)–B(2)	1.84(2)
Ru(3)–P	2.359(2)		
Ru(2)–Ru(1)–Ru(3)	57.2(1)	Ru(2)–Ru(1)–B(1)	51.7(5)
Ru(3)–Ru(1)–B(1)	75.6(4)	Ru(1)–Ru(2)–Ru(3)	66.0(1)
Ru(1)–Ru(2)–B(1)	52.9(4)	Ru(3)–Ru(2)–B(1)	81.5(3)
Ru(1)–Ru(2)–B(2)	81.2(5)	Ru(3)–Ru(2)–B(2)	53.5(4)
B(1)–Ru(2)–B(2)	48.6(6)	Ru(1)–Ru(3)–Ru(2)	56.9(1)
Ru(1)–Ru(3)–P	106.5(1)	Ru(2)–Ru(3)–P	159.1(1)
Ru(1)–Ru(3)–B(2)	74.7(5)	Ru(2)–Ru(3)–B(2)	51.2(4)
P–Ru(3)–B(2)	115.5(5)	Ru(1)–B(1)–Ru(2)	75.4(7)
Ru(1)–B(1)–B(2)	104.8(10)	Ru(2)–B(1)–B(2)	65.5(10)
Ru(2)–B(2)–Ru(3)	75.3(7)	Ru(2)–B(2)–B(1)	65.9(9)
Ru(3)–B(2)–B(1)	104.8(10)		

Table 7 Atomic coordinates ($\times 10^4$) for $[Ru_3(CO)_6(PPh_3)_3BH_5]$ **7**

Atom	x	y	z	Atom	x	y	z
Ru(1)	3 720(1)	8 429(1)	6 875(1)	C(35)	6 735(7)	6 756(5)	5 584(3)
Ru(2)	1 357(1)	8 092(1)	7 453(1)	C(36)	6 517(5)	7 128(5)	6 168(3)
Ru(3)	1 713(1)	10 088(1)	7 068(1)	C(41)	2 718(7)	5 295(5)	8 306(3)
P(1)	5 291(1)	6 916(1)	6 750(1)	C(42)	2 969(8)	4 282(5)	8 343(4)
P(2)	1 549(1)	7 169(1)	8 602(1)	C(43)	2 323(7)	3 742(5)	8 769(4)
P(3)	−296(1)	11 367(1)	7 009(1)	C(44)	1 423(7)	4 224(5)	9 157(4)
Cl(1)	4 848(3)	9 307(2)	838(1)	C(45)	1 172(6)	5 263(5)	9 125(3)
Cl(2)	5 503(3)	8 122(2)	2 196(1)	C(46)	1 805(6)	5 806(4)	8 689(3)
O(1)	5 355(5)	8 785(4)	7 926(2)	C(51)	−1 070(6)	7 565(5)	8 850(3)
O(2)	4 697(5)	9 693(4)	5 747(3)	C(52)	−2 157(7)	7 889(6)	9 177(4)
O(3)	−1 547(4)	8 976(4)	7 298(3)	C(53)	−2 095(7)	8 226(5)	9 760(4)
O(4)	1 188(6)	6 401(4)	6 804(3)	C(54)	−936(7)	8 235(5)	10 010(4)
O(5)	2 532(5)	10 525(4)	8 356(3)	C(55)	173(6)	7 901(5)	9 674(3)
O(6)	2 971(5)	11 539(4)	6 274(3)	C(56)	121(6)	7 566(4)	9 087(3)
C(1)	4 711(6)	8 641(4)	7 546(3)	C(61)	3 427(6)	6 354(5)	9 700(3)
C(2)	4 352(6)	9 223(5)	6 190(3)	C(62)	4 402(6)	6 383(5)	10 117(3)
C(3)	−445(6)	8 624(5)	7 364(3)	C(63)	4 833(6)	7 208(5)	9 996(3)
C(4)	1 302(6)	7 009(5)	7 056(3)	C(64)	4 290(6)	8 013(5)	9 476(3)
C(5)	2 262(6)	10 341(4)	7 867(3)	C(65)	3 319(6)	7 974(5)	9 060(3)
C(6)	2 484(6)	10 986(4)	6 559(3)	C(66)	2 863(5)	7 153(4)	9 161(3)
B(7)	1 487(6)	8 868(4)	6 380(3)	C(71)	−1 830(6)	12 462(5)	7 894(4)
C(8)	4 444(8)	9 166(7)	1 667(4)	C(72)	−2 378(7)	12 570(6)	8 496(4)
C(11)	3 850(8)	6 291(6)	5 910(4)	C(73)	−2 153(7)	11 749(6)	9 020(4)
C(12)	3 448(10)	5 602(8)	5 652(6)	C(74)	−1 369(7)	10 830(6)	8 944(3)
C(13)	3 880(11)	4 613(9)	5 943(6)	C(75)	−811(6)	10 701(5)	8 346(3)
C(14)	4 756(12)	4 285(7)	6 483(6)	C(76)	−1 044(6)	11 532(4)	7 803(3)
C(15)	5 192(9)	4 967(6)	6 734(4)	C(81)	650(6)	12 978(5)	7 026(4)
C(16)	4 739(6)	5 979(5)	6 450(3)	C(82)	785(7)	13 932(5)	6 791(4)
C(21)	7 597(6)	5 616(5)	7 476(3)	C(83)	117(8)	14 552(6)	6 213(4)
C(22)	8 359(7)	5 083(6)	8 048(4)	C(84)	−680(8)	14 214(5)	5 881(4)
C(23)	7 859(7)	5 128(5)	8 666(3)	C(85)	−823(7)	13 271(5)	6 105(3)
C(24)	6 597(6)	5 681(5)	8 715(3)	C(86)	−175(5)	12 643(4)	6 682(3)
C(25)	5 832(6)	6 204(5)	8 131(3)	C(91)	−1 319(6)	11 055(5)	5 852(3)
C(26)	6 329(5)	6 182(4)	7 508(3)	C(92)	−2 298(8)	11 012(6)	5 447(3)
C(31)	7 229(6)	7 731(6)	6 299(3)	C(93)	−3 528(7)	11 224(6)	5 629(4)
C(32)	8 164(7)	7 931(6)	5 886(4)	C(94)	−3 801(7)	11 484(7)	6 227(4)
C(33)	8 369(7)	7 538(6)	5 313(4)	C(95)	−2 862(6)	11 515(6)	6 658(3)
C(34)	7 654(8)	6 959(6)	5 169(4)	C(96)	−1 594(5)	11 315(4)	6 472(3)

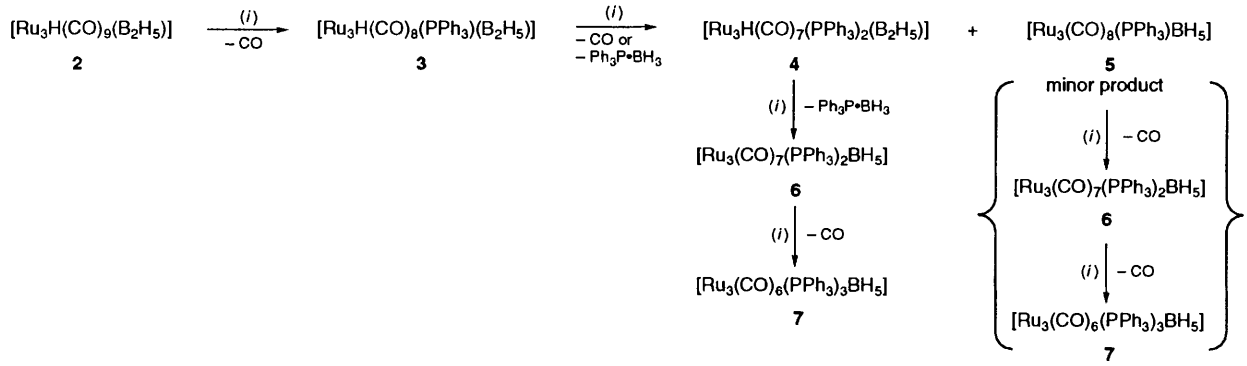

Scheme 1. Proposed pathways for the reaction of compound **2** with an excess of triphenylphosphine. Those shown in parentheses are not proven, but it is realistic to suggest that they occur as minor routes to clusters **6** and **7**. (*i*) PPh_3

Table 8 Selected bond distances (Å) and angles (°) for $[Ru_3(CO)_6(PPh_3)_3BH_5]$ **7**

Ru(1)–Ru(2)	2.952(1)	Ru(1)–Ru(3)	2.766(1)
Ru(2)–Ru(3)	2.921(1)	Ru(1)–B(7)	2.482(6)
Ru(2)–B(7)	2.264(6)	Ru(3)–B(7)	2.507(7)
Ru(1)–P(1)	2.353(2)	Ru(2)–P(2)	2.415(2)
Ru(3)–P(3)	2.355(1)	Ru(1)–H(1)	1.62(3)
B(7)–H(1)	1.46(2)	Ru(3)–H(2)	1.62(3)
B(7)–H(2)	1.48(2)	Ru(1)–H(3)	1.80(3)
Ru(2)–H(3)	1.81(3)	Ru(2)–H(4)	1.78(3)
Ru(3)–H(4)	1.78(3)	B(7)–H(7)	1.27(2)
Ru(1)–Ru(2)–Ru(3)	56.2(1)	Ru(1)–B(7)–Ru(2)	76.7(2)
Ru(2)–Ru(3)–Ru(1)	62.5(1)	Ru(3)–Ru(1)–Ru(2)	61.3(1)
Ru(2)–B(7)–Ru(3)	75.3(2)	Ru(1)–B(7)–Ru(3)	67.3(2)
Ru(2)–Ru(1)–P(1)	112.8(1)	Ru(3)–Ru(1)–P(1)	174.1(1)
Ru(2)–Ru(1)–B(7)	48.3(1)	Ru(3)–Ru(1)–B(7)	56.7(2)
P(1)–Ru(1)–B(7)	119.7(2)	Ru(1)–Ru(2)–P(2)	117.3(1)
Ru(3)–Ru(2)–P(2)	123.2(1)	Ru(1)–Ru(2)–B(7)	54.9(2)
Ru(3)–Ru(2)–B(7)	56.1(2)	P(2)–Ru(2)–B(7)	171.9(2)
Ru(1)–Ru(3)–P(3)	164.1(1)	Ru(2)–Ru(3)–P(3)	109.8(1)
Ru(1)–Ru(3)–B(7)	55.9(1)	Ru(2)–Ru(3)–B(7)	48.6(1)
P(3)–Ru(3)–B(7)	108.3(1)		

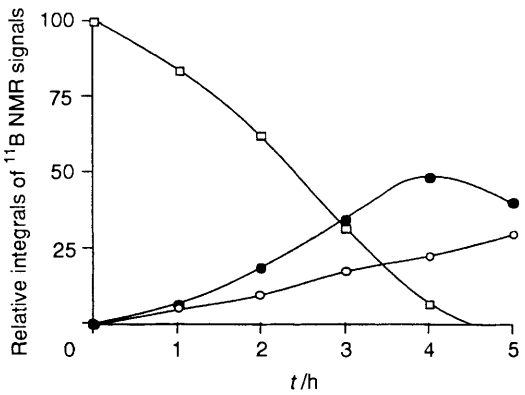

Fig. 3 Growth and decay of boron-containing components in the reaction of $[Ru_3H(CO)_8(PPh_3)(B_2H_5)]$ **3** (□) with an excess of PPh_3 in $[^2H_8]$thf monitored by ^{11}B NMR spectroscopy. ●, $[Ru_3H(CO)_7(PPh_3)_2(B_2H_5)]$ **4**; ○, $Ph_3P{\cdot}BH_3$

graph is constructed by using the integrals of the ^{11}B NMR resonances; we recognise that differences in relaxation times for the ^{11}B nuclei in different environments can lead to errors in interpreting the integrals in terms of the numbers of moles of compound present. However, we seek to gain an approximate mechanistic picture and have not attempted to use the data to analyse the kinetics of the reaction. The pattern for the production of Ru_3B clusters is derived by measuring the growth of $Ph_3P{\cdot}BH_3$. These data compare well with results obtained from ^1H NMR spectroscopy (Fig. 4) where each of the

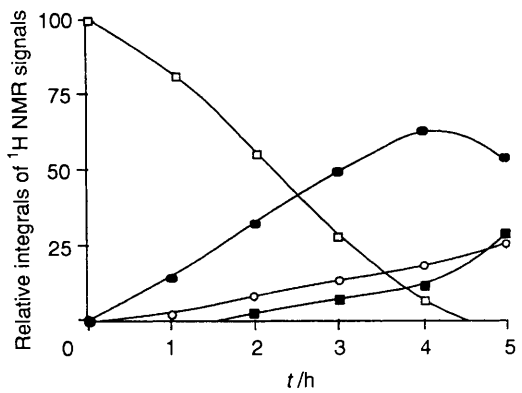

Fig. 4 Growth and decay of Ru_3B and Ru_3B_2 clusters in the reaction of $[Ru_3H(CO)_8(PPh_3)(B_2H_5)]$ **3** (□) with an excess of PPh_3 in $[^2H_8]$thf monitored by ^1H NMR spectroscopy. ●, $[Ru_3H(CO)_7(PPh_3)_2(B_2H_5)]$ **4**; ○, $[Ru_3(CO)_7(PPh_3)_2BH_5]$ **6**; ■, $[Ru_3(CO)_6(PPh_3)_3BH_5]$ **7**

compounds **3**–**7** can be distinguished. Note that in the reaction of **3** with PPh_3 the monosubstituted cluster **5** is not formed in significant quantities.

Inspection of Figs. 3 and 4 shows that the amount of compound **4** grows initially but then begins to decay indicating that it is a precursor to some, at least, of clusters **6** and **7**. The rate of formation of the Ru_3B clusters **6** and **7** over the 5 h reaction period is less than the initial rate of formation of **4**. The ^1H NMR spectral data illustrate that trisubstituted **7** is only formed once some disubstituted **6** is present in the system. No trisubstituted derivative of formula $[Ru_3H(CO)_6(PPh_3)_3(B_2H_5)]$ was ever observed and this suggests that the abstraction of BH_3 from disubstituted **4** is quite facile; cluster degradation competes with phosphine-for-carbonyl substitution at the expense of the latter pathway.

The above results, taken in conjunction with the results from the stoichiometric reaction of compound **2** with PPh_3, lead us to propose that the substitution and degradation pathways follow the sequence shown in Scheme 1. The initial reaction of **2** with PPh_3 follows a substitution pathway to yield **3**. Then, reaction of **3** with PPh_3 follows one of two competitive pathways, substitution or abstraction of BH_3, the former, to give **4**, being the dominant route. Abstraction of BH_3 followed by phosphine-for-carbonyl substitution then occur. A significant observation which underlines the relatively robust nature of the triruthenaborane clusters is that the Ru_3B clusters are not apparently degraded by PPh_3 to non-boron triruthenium-based products. This is in marked contrast to the facile abstraction of monoborane from $[Fe_3(CO)_9(BH_4)]^-$ on treatment with Lewis bases.[26,27]

Acknowledgements

We thank the Donors of the Petroleum Research Fund,

administered by the American Chemical Society, for support of this research (grants 22771-AC3 and 25533-AC3), the SERC for a studentship (to D. M. M.) and to the National Science Foundation for a grant (CHE9007852) towards the purchase of a diffractometer at the University of Delaware.

References

1 A. K. Chipperfield and C. E. Housecroft, *J. Organomet. Chem.*, 1988, **349**, C17.
2 A. K. Chipperfield, C. E. Housecroft and D. M. Matthews, *J. Organomet. Chem.*, 1990, **384**, C38.
3 C. E. Housecroft, D. M. Matthews and A. L. Rheingold, *J. Chem. Soc., Chem. Commun.*, 1992, 323.
4 J. C. Vites, C. E. Housecroft, C. Eigenbrot, M. L. Buhl, G. J. Long and T. P. Fehlner, *J. Am. Chem. Soc.*, 1986, **108**, 3304.
5 S. M. Draper, C. E. Housecroft, A. K. Keep, D. M. Matthews, X. Song and A. L. Rheingold, *J. Organomet. Chem.*, 1992, **423**, 241.
6 C. E. Housecroft, D. M. Matthews, A. L. Rheingold and X. Song, *J. Chem. Soc., Dalton Trans.*, 1992, 2855.
7 E. Benedetti, M. Biachi, P. Frediani and F. Piacenti, *Inorg. Chem.*, 1971, **10**, 2759.
8 A. D. Hattersley, C. E. Housecroft, J. S. Humphrey and D. M. Matthews, unpublished work.
9 G. M. Sheldrick, SHELXTL 5.1, Nicolet (Siemens), Madison, WI.
10 C. R. Eady, B. F. G. Johnson and J. Lewis, *J. Chem. Soc., Dalton Trans.*, 1977, 477.
11 T. P. Fehlner, in *Boron Chemistry*, eds. R. W. Parry and G. Kodama, Pergamon, Oxford, 1980, p. 95.
12 T. P. Fehlner, *Adv. Inorg. Chem.*, 1990, **35**, 199.
13 V. R. Miller and R. N. Grimes, *J. Am. Chem. Soc.*, 1973, **95**, 5078.
14 N. N. Greenwood, C. G. Savory, R. N. Grimes, L. G. Sneddon, A. Davison and S. S. Wreford, *J. Chem. Soc., Chem. Commun.*, 1974, 718.
15 L. G. Sneddon and D. Voet, *J. Chem. Soc., Chem. Commun.*, 1976, 118.
16 T. L. Venable and R. N. Grimes, *Inorg. Chem.*, 1982, **21**, 887.
17 E. L. Andersen, K. J. Haller and T. P. Fehlner, *J. Am. Chem. Soc.*, 1979, **101**, 4390.
18 K. J. Haller, E. L. Andersen and T. P. Fehlner, *Inorg. Chem.*, 1981, **20**, 309.
19 See, for example, J. R. Shapley, S. I. Richter, M. R. Churchill and R. A. Lashewycz, *J. Am. Chem. Soc.*, 1977, **99**, 7384.
20 W. J. Dulmange and W. N. Lipscomb, *Acta Crystallogr.*, 1952, **5**, 260; D. Schwoch, A. B. Burg and R. A. Beaudet, *Inorg. Chem.*, 1977, **16**, 3219; R. Greatrex, N. N. Greenwood, D. W. H. Rankin and H. E. Robertson, *Polyhedron*, 1987, **6**, 1849 and refs. therein.
21 C. E. Housecroft, *Adv. Organomet. Chem.*, 1991, **33**, 1.
22 T. P. Fehlner, *New J. Chem.*, 1988, **12**, 307.
23 D. P. Workman and S. G. Shore in *Electron Deficient Boron and Carbon Clusters*, eds. G. A. Olah, K. Wade and R. E. Williams, Wiley, New York, 1991, pp. 237–260.
24 T. P. Fehlner and N. P. Rath, *J. Am. Chem. Soc.*, 1988, **110**, 5345; T. P. Fehlner, P. T. Czech and R. F. Fenske, *Inorg. Chem.*, 1990, **29**, 3103; R. Khattar, T. P. Fehlner and P. T. Czech, *New J. Chem.*, 1992, **15**, 705.
25 H. Nöth and B. Wrackmeyer, *Nuclear Magnetic Resonance Spectroscopy of Boron Compounds*, Springer, Berlin, 1978, ch. 2.
26 C. E. Housecroft and T. P Fehlner, *Inorg. Chem.*, 1986, **25**, 404.
27 C. E. Housecroft and T. P. Fehlner, *J. Am. Chem. Soc.*, 1986, **108**, 4867.

Received 27*th April* 1993; *Paper* 3/02420B